Available online at www.sciencedirect.com
ScienceDirect
Journal of Magnetism and Magnetic Materials 312 (2007) 1–5
Journal of magnetism and magnetic materials
www.elsevier.com/locate/jmmm

Studies on the magnetic properties for single-phase nanocrystalline FePt magnets with different orientation degrees

Shu-li He[a,b,*], Hong-wei Zhang[b], Chuan-bing Rong[b], Ren-jie Chen[b], Ji-rong Sun[b], Bao-gen Shen[b]

[a]*Department of Physics, Capital Normal University, Beijing 100037, China*
[b]*State Key Laboratory of Magnetism, Institute of Physics, Chinese Academy of Science, Beijing 100080, China*

Received 24 March 2006; received in revised form 7 August 2006
Available online 28 September 2006

Abstract

The single-phase nanocrystalline FePt magnets composed of 343 irregular-shaped grains are built. The demagnetization curves are simulated by micromagnetic finite element method. The remanence, coercivity and maximum energy product of the magnets decrease with deteriorating grain alignment. The characteristics of variation of magnetic properties with the degree of orientation are closely related to the average grain size of nanocrystalline magnets. The contribution of intergrain exchange coupling (IGEC) to remanence enhancement is associated to the degree of orientation, and decreases with improved grain alignment. With decreasing grain size, coercivity increases for anisotropic nanocrystalline magnets, which is completely different from that of isotropic nanocrystalline magnets.

PACS: 75.50.Ww; 75.50.Tt; 75.60.Jk

Keywords: FePt nanocrystalline magnets; Remanence; Coercivity; Micromagnetic finite-element method; Permanent magnet

1. Introduction

FePt alloys with the $L1_0$ ordered structure have attracted much attention because of their potential applications in ultrahigh-density magnetic recording [1–3]. The ordered phase of FePt system possesses high magnetocrystalline anisotropy and allows the use of thermally stable particles of 3–4 nm in diameter as the basic unit for recording [4]. In addition, FePt alloys are attractive as permanent magnets because of their satisfactory mechanical strength and good chemical stability [5,6]. In the past decades, the hard magnetic properties of FePt alloys have been studied extensively [7–9]. However, little work has been done on nanoscaled FePt systems. Recently, chemical method reported by the IBM group [10–13] make it possible to use nanostructured FePt for potential permanent magnet applications due to its advantages of highly controllable particle size, size distribution and chemical composition. Zeng et al. [14] reported FePt/Fe_3Pt nanocomposite magnets with the mean grain size of 5 nm synthesized by a chemical method, which exhibit an energy product of 20.1 MGOe. Although the grain size of nanocomposite magnets has been reduced to less than 10 nm, the energy product of magnets is far bellow the magic number of 144 MGOe predicted by Skomski and Coey [15]. Therefore, improved alignment of the axes of the hard grains becomes attractive to exploit the full magnetic potential of the nanostructured permanent magnets.

A series of nanocrystalline magnets with different degrees of orientation are very difficult to prepare using the existing experimental techniques. However, the micromagnetic finite-element method (FEM) is effective for the simulation of hysteretic behaviour where thermal activation is ignored [16–20]. Zhang et al. [19] have checked the contribution of thermal activation by experiments. In their work, $Pr_{12}Fe_{82}B_6$ ribbons were measured after waiting for 1 and 2000 s when the field reached the expected value. A thermal activation was found at room temperature, but the change of coercivity was much smaller than the

*Corresponding author. Department of Physics, Capital Normal University, Beijing 100037, China. Tel.: +86 10 68982268; fax: +86 10 68902347.
E-mail address: hsl-phy@163.com (S.-l. He).

0304-8853/$ - see front matter © 2006 Elsevier B.V. All rights reserved.
doi:10.1016/j.jmmm.2006.08.039

corresponding coercivity. Therefore, the thermal activation can be approximately ignored at room temperature. In this paper, single-phase FePt nanostructured magnets with different degrees of orientation are built and the demagnetization behaviour of magnets is investigated by micromagnetic FEM.

2. Simulation model

The numerical simulation model used to investigate magnetization processes in ferromagnetics is based on the continuum theory of micromagnetics. By means of FEM, the total magnetic Gibbs free energy,

$$G = E_H + E_D + E_k + E_{ex},$$

is minimized with respect to the direction of the spontaneous polarization J_s. Here, E_H is the Zeeman energy in an external field, E_D the dipolar interaction energy, E_k the anisotropy energy and E_{ex} the exchange energy. In numerical calculations, dipolar interaction is taken into consideration by introducing a magnetic vector potential. A more detailed description of the simulation method used has been given in Ref. [21].

The samples are composed of 343 irregular shaped grains with an average diameter from 3 to 10 nm as shown in Fig. 1. In the case of uniaxial materials, the misalignment of a grain may be described by the angle θ between the c-axis and the average alignment direction. The degree of orientation is characterized by the standard deviation:

$$\sigma = \frac{1}{N}\sqrt{\sum_{i=1}^{N}(\theta_i - \overline{\theta})^2},$$

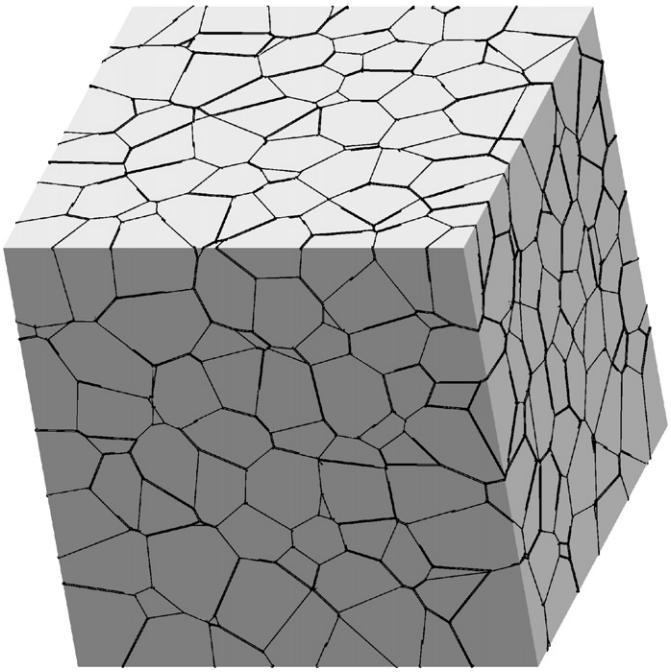

Fig. 1. Samples composed of 343 irregularly shaped grains.

where $\overline{\theta}$ denotes the average direction of easy axes and θ_i denotes the angle between the local easy axis direction and $\overline{\theta}$. The external field H_{ex} is applied parallel to the z-direction which is defined identical with the preferred alignment axis, i.e. $\overline{\theta} = 0$. According to experimental studies [22], we use Gaussian distribution function for the easy axes of oriented magnets:

$$f_{Gauss}(\theta) \sim e^{-(\theta^2/2\sigma'^2)},$$

where σ' is not identical with the standard deviation like usually for Gaussian function because of the cutoff of the distribution function for the angles $\theta_i > 90^\circ$.

The magnetic parameters used for the calculation at room temperature are as follows:

$J_s = 1.38\,T$, $K_1 = 6.63 \times 10^6\,J/m^3$ and $A = 1.03 \times 10^{-11}\,J/m$. Thus, the Bloch domain wall width is $\delta_B = 3.7\,nm$ and the anisotropy field is $\mu_0 H_A = 12\,T$. In calculations, 90,000–120,000 elements are used.

3. Results and discussion

3.1. Remanence

The dependence of reduced remanence m_r on the standard deviation σ of $f(\theta)$ is shown in Fig. 2(a). Fig. 2(a) demonstrates that m_r of ideally orientated magnets ($\sigma = 0$) is 1.0, which suggests that all the magnetizations in the perfectly orientated magnets are parallel to the direction of H_{ex} in remanent state. It is also found that the value of m_r is far larger than 1/2. The competition between magnetocrystalline anisotropy and exchange interaction causes a smooth transition of magnetization from one easy direction to the other over a width of δ_B. With deteriorated grain alignment, the number of local easy axes deviating from the direction of H_{ex} increases, which results in a reduction of remenance. Therefore, m_r of magnets reduces monotonically with increasing σ as described in Fig. 2(a).

Fig. 2(a) also shows the dependence of m_r on standard deviation σ in the Stoner–Wohlfarth model. A rapid reduction is obviously found in the ensemble of non-interaction particles. In nanocrystalline permanent magnets (NPMs), neighbouring grains coupled by exchange interactions tend to align their magnetization parallel to each other, which leads to remanence enhancement [23,24]. So, NPMs should show stronger remanence enhancement than ensemble of non-interaction particles with the same degree of orientation. Remanence enhancement in orientated NPMs is contributed by both the orientation of local easy axes and intergrain exchange coupling (IGEC).

The contribution of IGEC to m_r in magnets with different degrees of orientation is calculated as shown in Fig. 2(b). It can be seen that the contribution of IGEC to m_r decreases with improving alignment of easy axes. In the perfectly orientated magnets, the contribution of IGEC to m_r is nearly zero and calculations confirm that the value of

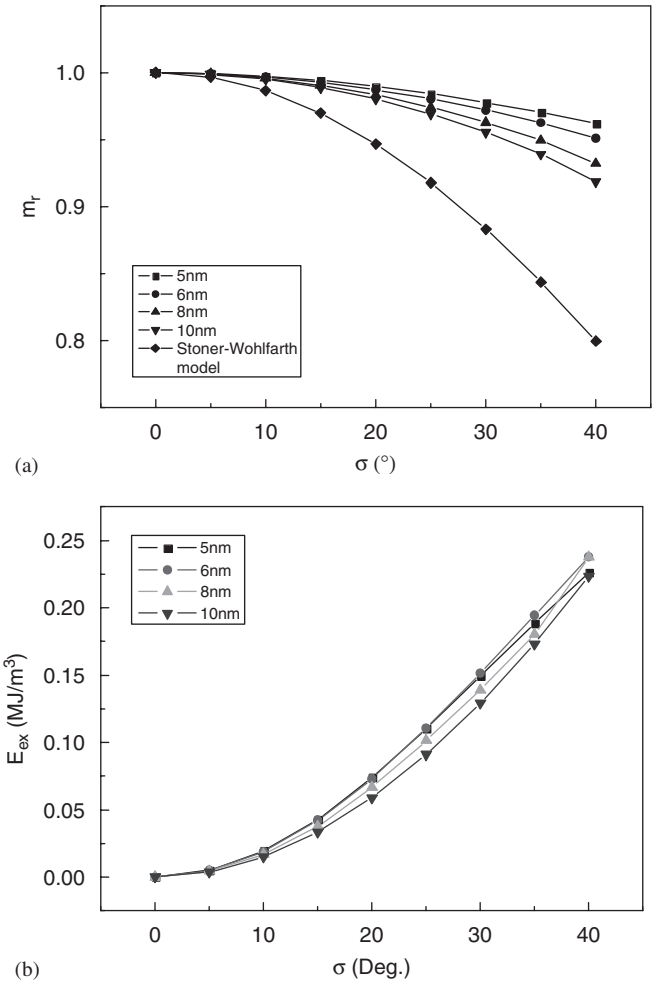

Fig. 2. Dependence of reduced remanence m_r on the standard deviation σ of $f(\theta)$ (a) and Contribution of IGEC to m_r in magnets with different degree of orientation (b).

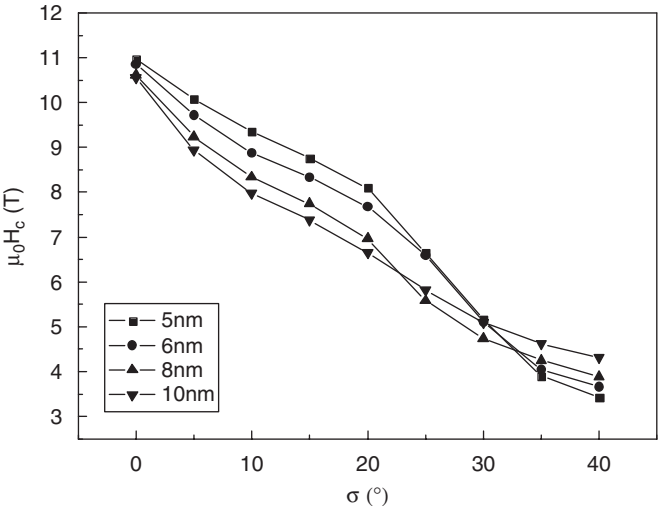

Fig. 3. Coercivity as a function of standard deviation σ of $f(\theta)$ for magnets with different grain size.

E_{ex} is very small. In NPMs, IGEC is affected strongly by the mean grain size. The smaller the average grain diameter, the stronger is IGEC and the larger the fraction of interaction areas.

3.2. Coercivity

Fig. 3 shows the dependence of coercivity H_c on the standard deviation σ for magnets with different grain size. H_c decreases monotonously with increasing σ for magnets with a grain size of 3–10 nm. In NPMs, the following micromagnetics-based equation for the coercivity field is proposed:

$$H_c = 2\alpha_k\alpha_\phi\alpha_{ex}H_N - N_{eff}J_s/\mu_0, \quad (1)$$

where α_k is a microstructural parameter taking into account the reduced surface anisotropy of nonperfect grains; α_φ is a parameter considering the misalignment of the grains in the magnets, which is equal to 0.5 for isotropic permanent magnet (PM) and 1 for perfectly oriented PM; α_{ex} is a dimensionless microstructural parameter dependent on the effect of the exchange coupling between neighbouring grains; N_{eff} is an effective demagnetization factor describing the internal stray fields acting on the grains. In our calculation, α_k is equal to 1 due to perfect intergranular layers in our models. According to Eq. (1), coercivity field increases with improving grain alignment, which is coincident with the result of Fig. 3.

It should be mentioned that H_c of orientated NPMs increases with decreasing grain size in the case of $\sigma \leqslant 20$, which is completely different from that of isotropic NPMs [25,26]. IGEC forces magnetization to deviate somewhat from the local easy axis in NPMs. It not only leads to remanence enhancement, but also results in nucleation field diminution. Therefore, H_c of exchange-coupled PM is always smaller than that of decoupled PM. The stronger the IGEC, the smaller the H_c of NPMs. In orientated NPMs, H_c is affected not only by the grains alignment, but also by the strength of IGEC. The following formula is attempted to describe H_c in orientated NPMs:

$$H_c = H_{ex} + H_{\alpha\phi}. \quad (2)$$

Here, H_{ex} denotes the contribution of IGEC to H_c and $H_{\alpha\varphi}$ describes the contribution of grain alignment in the Stoner–Wohlfarth model. The Stoner–Wohlfarth model suggests nucleation field H_N as the following equation [27]:

$$H_N = \frac{2K_1}{J_S\cos\phi(1+\tan^{2/3}\phi)^{3/2}}. \quad (3)$$

Here ϕ is the orientation angle of the magnetic field. It can be deduced from Eq. (3) that, with increasing ϕ, H_N decreases rapidly in the case of $\phi \leqslant 40^\circ$. According to Eq. (1), $H_{\alpha\varphi}$ increases with improving grain alignment and is positive all the time in our calculations. H_{ex} of anisotropic nanoscaled magnets is significantly affected by both IGEC and grain alignment, and varies from positive to negative value with deteriorating grain alignment.

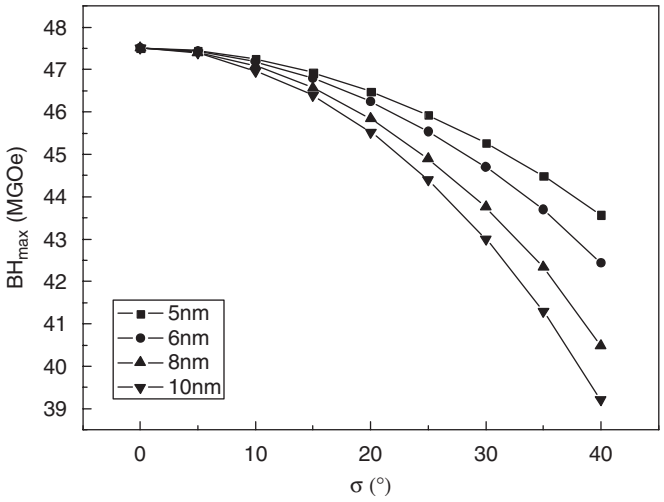

Fig. 4. $(BH)_{max}$ as a function of standard deviation σ of $f(\theta)$ for magnets with different grain size.

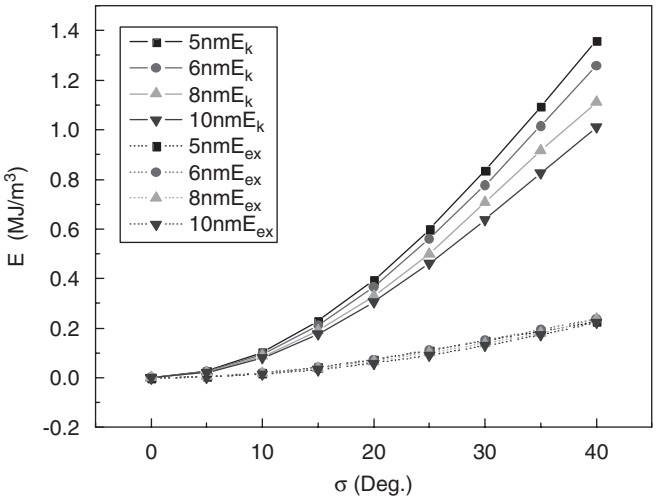

Fig. 5. Dependence of exchange energy E_{ex} and anisotropy energy E_k on standard deviation σ for magnets with different grain size at remanent state.

3.3. Maximum energy product

Fig. 4 summarizes the maximum energy product $(BH)_{max}$ as a function of the standard deviation σ for the magnets with different grain size, which is very similar to the result of Fig. 2. As the coercivity field of the calculated magnets is higher than one-half of the remanence, $(BH)_{max}$ sensitively depends on the remanence according to the theoretical upper limit of isotropic samples:

$$(BH)_{max} = \frac{1}{4\mu_0} J_r^2. \quad (4)$$

This result agrees with an enhancement of $(BH)_{max}$ with increasing remanence.

3.4. Exchange and anisotropy energy at remanent state

Fig. 5 shows the dependence of exchange energy E_{ex} and anisotropy energy E_k on the standard deviation σ for the magnets with different grain size at remanent state. It is clear that both E_{ex} and E_k reduce monotonically with improving orientation of magnets. For the perfectly oriented magnets, both E_{ex} and E_k are approximately zero at the remanent state. According to the expression of E_{ex} in micromagnetism [28,29], E_{ex} is related to the angle between the neighbouring grains. For the ideally orientated magnets, magnetization vectors in the grains are all parallel to the direction of applied field at remanent state, i.e. all the angles between the neighbouring grains is zero. At the same time, all the local easy axes of the perfectly orientated magnets are parallel to the direction of applied field. The number of local easy axes which deviate from z-direction increases with increasing σ. On the other hand, IGEC forces magnetization to somewhat deviate from the local easy axes, which results in an enhancement of E_k with increasing σ.

4. Conclusions

The orientated NPMs show high remanence due to the contribution of both IGEC and improved grain alignment. The value of remanence is determined by the competition of exchange energy E_{ex} and anisotropy energy E_k at room temperature. As the neighbouring grains are coupled by strong exchange interaction in FePt magnets with the grain sizes of several nanometres, E_k increases more rapidly with the deterioration of grain alignment than E_{ex}. The contribution of IGEC to coercivity is complicated, which is positive for the magnets with perfect orientation of easy axes and varies from positive to negative with deteriorating grain alignment. IGEC plays an important role in the magnetic properties of nanoscaled permanent magnets with the orientation of grain alignment.

Acknowledgements

This work was supported by the Science Foundation of Education Commission of Beijing.

References

[1] K. Inomata, T. Sawa, S. Hashimoto, J. Appl. Phys. 64 (1988) 2537.
[2] D. Weller, A. Moser, IEEE Trans. Magn. 35 (1999) 4423.
[3] D. Weller, L. Folks, M.E. Best, L. Wen, M.F. Toney, M. Schwickert, J.U. Thiele, M.F. Doerner, IEEE Trans. Magn. 36 (2000) 10.
[4] R.F.C. Farrow, J. Appl. Phys. 79 (1996) 5967.
[5] S.H. Liu, IEEE Trans. Magn. 35 (1999) 3989.
[6] Q. Squalli, M.P. Brenal, P. Hoffmann, F. Weible-Marquis, Appl. Phys. Lett. 76 (20000) 2134.
[7] A.D. Franklin, A.E. Berkowitz, E. Klokholm, Phys. Rev. 94 (1954) 1423.
[8] K. Watanabe, H. Masumoto, Trans. Jpn. Inst. Met. 24 (1983) 627.
[9] S.W. Yung, Y.H. Chang, T.J. Lin, M.P. Hung, J. Magn. Magn. Mater. 116 (1992) 411.
[10] S. Sun, C.B. Murray, D. Weller, L. Folks, A. Moser, Science 287 (2000) 1989.

[11] S. Sun, E.E. Fullerton, D. Weller, C.B. Murray, IEEE Trans. Magn. 37 (2001) 1239.
[12] H. Zeng, S. Sun, T.S. Vedantam, J.P. Liu, Z.R. Dai, Z.L. Wang, Appl. Phys. Lett. 80 (2002) 2583.
[13] M. Chen, J.P. Liu, S. Sun, J. Am. Chem. Soc. 126 (2004) 8394.
[14] H. Zeng, J.P. Liu, Z.L. Wang, S. Sun, Nature 420 (2002) 395.
[15] R. Skomski, J.M.D. Coey, Phys. Rev. B 48 (1993) 15812.
[16] R. Fischer, T. Leineweber, H. Kronmuller, Phys. Rev. B 57 (1998) 10723.
[17] H. Kronmuller, R. Fischer, M. Bachmann, T. Leineweber, J. Magn. Magn. Mater. 203 (1999) 12.
[18] R. Fischer, H. Kronmuller, J. Appl. Phys. 83 (1998) 3271.
[19] H.W. Zhang, C.B. Rong, X.B. Du, S.Y. Zhang, B.G. Shen, J. Magn. Magn. Mater. 278 (2004) 127.
[20] H.W. Zhang, C.B. Rong, X.B. Du, J. Zhang, S.Y. Zhang, B.G. Shen, Appl. Phys. Lett. 82 (2003) 4098.
[21] R. Fischer, H. Kronmuller, Phys. Rev. B 54 (1996) 7284.
[22] F. Vial, F. Joiy, E. Nevalainen, M. Sagawa, K. Hiraga, K.T. Park, J. Magn. Magn. Mater. 242 (2002) 1329.
[23] R. Fischer, T. Schrefl, H. Kronmuller, J. Fidler, J. Magn. Magn. Mater. 153 (1996) 35.
[24] J. Bauer, M. Seeger, A. Zern, H. Kronmuller, J. Appl. Phys. 80 (1996) 1667.
[25] H.W. Zhang, C.B. Rong, J. Zhang, S.Y. Zhang, B.G. Shen, Phys. Rev. B 66 (2002) 184436.
[26] W.Y. Zhang, C.B. Rong, J. Zhang, B.G. Shen, H.L. Du, J.S. Jiang, Y.C. Yang, J. Appl. Phys. 92 (2002) 7647.
[27] E.C. Stoner, E.P. Wohlfarth, Phil. Trans. Roy. Soc. (London) 240 (1948) 599.
[28] W.F. Brown Jr., Phys. Rev. 58 (1940) 736.
[29] W.F. Brown Jr., Phys. Rev. 124 (1961) 1348.